AGU PUBLICATIONS

Geophysical Research Letters

RESEARCH LETTER
10.1002/2015GL063541

Key Points:
- Metamorphism was followed with a cryo-cell operating at room temperature
- The −2°C anisotropic faceting behavior of ice was observed in 3D
- High-technology imaging is now accessible to the dynamic 3-D study of snow

Correspondence to:
N. Calonne and F. Flin,
neige.calonne@gmail.com;
frederic.flin@meteo.fr

Citation:
Calonne, N., et al. (2015), CellDyM: A room temperature operating cryogenic cell for the dynamic monitoring of snow metamorphism by time-lapse X-ray microtomography, *Geophys. Res. Lett.*, *42*, 3911–3918, doi:10.1002/2015GL063541.

Received 26 FEB 2015
Accepted 6 APR 2015
Accepted article online 13 APR 2015
Published online 18 MAY 2015

©2015. American Geophysical Union. All Rights Reserved.

CellDyM: A room temperature operating cryogenic cell for the dynamic monitoring of snow metamorphism by time-lapse X-ray microtomography

N. Calonne[1,2,3], F. Flin[1], B. Lesaffre[1], A. Dufour[1], J. Roulle[1], P. Puglièse[1], A. Philip[1], F. Lahoucine[4], C. Geindreau[2,3], J.-M. Panel[1], S. Rolland du Roscoat[2,3], and P. Charrier[2,3]

[1]Météo-France—CNRS, CNRM—GAME UMR 3589, CEN, Saint Martin d'Hères, France, [2]Université Grenoble Alpes, Laboratoire 3SR, Grenoble, France, [3]CNRS, Grenoble, France, [4]Concept Soudure, Echirolles, France

Abstract Monitoring the time evolution of snow microstructure in 3-D is crucial for a better understanding of snow metamorphism. We, therefore, designed a cryogenic cell that precisely controls the experimental conditions of a sample while it is scanned by X-ray tomography. Based on a thermoelectrical regulation and a vacuum insulation, the cell operates at room temperature. It is, thus, adaptable to diverse scanners, offering advantages in terms of imaging techniques, resolution, and speed. Three-dimensional time-lapse series were obtained under equitemperature and temperature gradient conditions at a 7.8 μm precision. The typical features of each metamorphism and the anisotropic faceting behavior between the basal and prismatic planes, known to occur close to −2°C, were observed in less than 30 h. These results are consistent with the temperature fields expected from heat conduction simulations through the cell. They confirm the cell's accuracy and the interest of relatively short periods to study snow metamorphism.

1. Introduction

Snow metamorphism strongly influences the snow properties, which are critical for applications such as snowpack stability [*Schweizer et al.*, 2003], transport of chemical species [*Grannas et al.*, 2007], and snow energy balance [*Sokratov and Barry*, 2002]. However, some of the physical mechanisms involved in metamorphism are still not fully understood and need further investigations. Three-dimensional (3-D) images of snow make the quantitative study of the metamorphism possible by providing the precise evolution of the microstructures with time [e.g., *Flin et al.*, 2004; *Schneebeli and Sokratov*, 2004; *Kämpfer and Schneebeli*, 2007; *Pinzer and Schneebeli*, 2009a; *Chen and Baker*, 2010; *Srivastava et al.*, 2010; *Pinzer et al.*, 2012; *Calonne et al.*, 2014a]. Such images generally correspond to representative elementary volumes of the snow layers from which they are taken and thus can be used to compute effective physical properties of snow arising in macroscopic models [e.g., *Calonne et al.*, 2011; *Zermatten et al.*, 2011; *Riche and Schneebeli*, 2013; *Calonne et al.*, 2012; *Löwe et al.*, 2013; *Calonne et al.*, 2014a, 2014b; *Zermatten et al.*, 2014]. For these reasons, several methods have been developed in the last 15 years to obtain 3-D images of snow by X-ray microtomography. Up to now, two different approaches have been used: a static and a dynamic approach.

The static approach aims at imaging a snow sample whose structural evolution has been stopped before the tomographic acquisition [e.g., *Brzoska et al.*, 1999; *Coléou et al.*, 2001; *Flin et al.*, 2004; *Heggli et al.*, 2009; *Calonne et al.*, 2014a]. To do so, the impregnation technique is generally used: the porosity of the snow sample is filled by a product that is liquid below 0°C, and the whole is then refrozen at a lower temperature. The impregnation has two effects: it stops the metamorphism and consolidates the sample for further transportation or machining of subsamples. This method is intended to preserve exactly the sampled microstructure until the tomography. It is thus especially appropriate for the sampling of snow specimens on the field. With this approach, the metamorphism of a homogeneous snow slab can be monitored by imaging different snow samples collected at several time intervals in the slab [*Flin et al.*, 2004; *Srivastava et al.*, 2010; *Calonne et al.*, 2014a]. However, this approach is not suited to time-lapse imaging, since each stage of the metamorphism corresponds to a different sample. The tomography takes place either in a cold room or in an ambient temperature room. In the latter case, this approach requires a cryogenic cell to protect the snow sample from outside's conditions during the scan. A precise control of the temperature is not needed, the goal being only to keep the sample in a sufficiently cold environment to prevent any phase change of the considered

materials during a scan. This is one of the main advantages of the static method: it can be applied on various X-ray scanners operating at room temperature by using a quite simple cryogenic cell [*Coléou et al.*, 2001; *Miedaner et al.*, 2007; *Calonne et al.*, 2014a].

The dynamic approach consists of scanning the same nonimpregnated sample while it undergoes structural evolutions under specific conditions of metamorphism [e.g., *Schneebeli and Sokratov*, 2004; *Pinzer and Schneebeli*, 2009a; *Chen and Baker*, 2010]. The main difficulty of this approach is the precise control of the temperature conditions within a small snow sample for long time periods. To facilitate this temperature control, the whole experiment occurs, up to now, in cold room and the sample is scanned by a dedicated cold room tomograph. Even in cold room, the use of a cryogenic cell [*Pinzer and Schneebeli*, 2009b] is generally required to precisely control the temperature conditions at the boundaries of the sample during the experiment. The dynamic approach has some drawbacks inherent to the use of laboratory tomographs, which may induce several limitations in terms of imaging technology. However, this approach gives access to the grain to grain evolution of a same snow sample by time-lapse tomography. Such time series of 3-D images provide important information on the ice growth processes and the vapor transfers involved [*Pinzer et al.*, 2012] and are crucial for microscopic models of metamorphism [e.g., *Flin et al.*, 2003; *Kämpfer and Plapp*, 2009].

Trying to combine the advantages of the static and dynamic approaches, *Enzmann et al.* [2011] and *Rolland du Roscoat et al.* [2011] designed experiments to monitor the evolution of the same sample using a cryo-cell operating at room temperature. However, these experiments do not really allow a long-term and undisturbed monitoring of snow metamorphism. Indeed, using a cell developed for the static approach [*Miedaner et al.*, 2007], *Enzmann et al.* [2011] focused on the evolution of tiny internal bubbles contained in graupel particles and limited their observation to two image acquisitions (at −60°C), separated by 30 min, of metamorphism at −8°C. Such a procedure required changes of temperature conditions between the acquisitions, which do not really allow monitoring of the metamorphism under stable and well-defined conditions. In addition, due to the strong evolution of the microstructure observed under thermal cycling, the authors have pointed out the difficulty of adequately preserving the sample before its installation into the cell. Similarly, *Rolland du Roscoat et al.* [2011], who were interested in monitoring the crystalline behavior of large snow grains under slow compression tests, restricted their observations to short periods of time (a few hours) and noticed several difficulties concerning the humidity and thermal regulation, in spite of the specifically developed cell. Actually, due to their technical designs (e.g., liquid nitrogen use and/or asymmetrical temperature regulation systems), both of these cells would fail in maintaining any typical snow sample in well-controlled conditions over several hours.

We designed a new cryogenic cell that is suited to the dynamic approach, operates at room temperature, and solves the above mentioned problems. This cell, called Cell for Dynamic Monitoring (CellDyM), includes the main advantages of the above approaches: (1) It enables the grain to grain monitoring of a same snow sample during several days of metamorphism by precisely regulating the temperature conditions at the boundaries of the sample. (2) It can be adapted to a large panel of scanners operating at room temperature, including those of synchrotron instruments. This provides new opportunities, in terms of imaging techniques, resolution, and speed [e.g., *Rolland du Roscoat et al.*, 2011; *Nguyen-Thi et al.*, 2012] to the dynamic study of snow metamorphism.

2. Description of the Cryogenic Cell

This work was motivated by the need to monitor snow metamorphism by time-lapse microtomography with a scanner operating at room temperature. For that purpose, we designed the CellDyM to precisely impose the temperature conditions at the top and bottom of the sample while its lateral sides are thermally insulated from the outside. Specific requirements for the cell's design concerned the X-ray absorption properties of the materials that must ensure a good contrast of the air and ice on the reconstructed images, the size of the snow sample that must be large enough to be representative, and the geometrical arrangement of the cell that must enable a 360° rotation during a tomographic acquisition. In addition, the snow sample must be protected from heating and frosting during its installation within the cell for the tomography, and the setting up must be fast (see section 4). Figure 1 presents a schematic of the CellDyM, which can be decomposed into three functional parts: (1) a system of cold production and regulation that controls the temperature gradient (TG) imposed on the sample, (2) a removable conduction system that conducts heat from the cold production

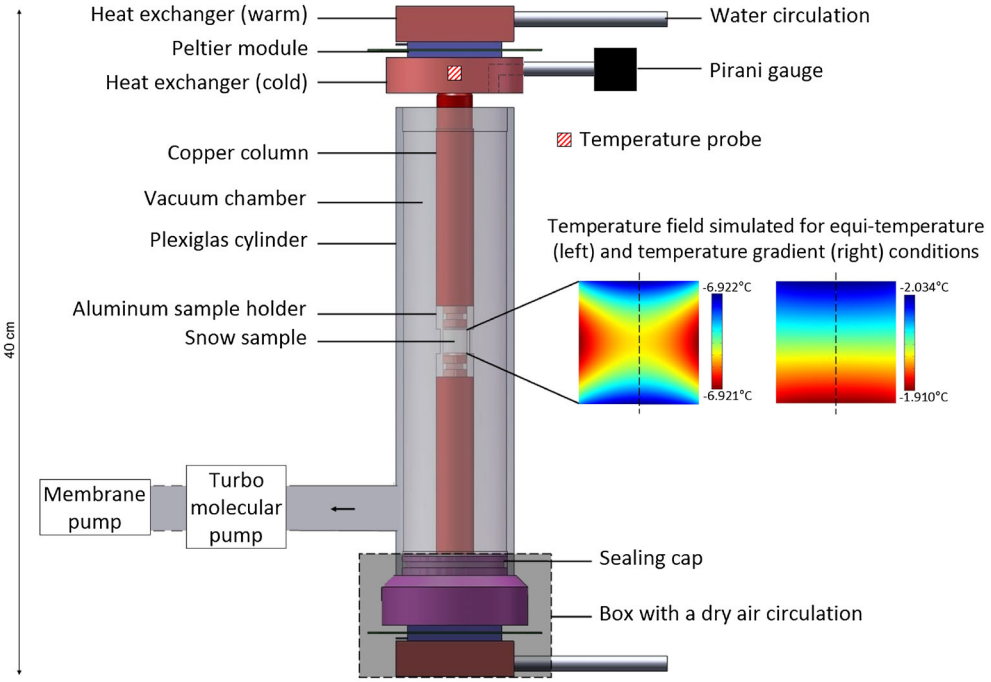


Figure 1. Schematic of the CellDyM and simulations of the temperature field within the snow sample. All the components situated on both extremities of the snow sample are strictly identical, with the exception of the vacuum pumping system located at the base of the Plexiglas cylinder and the vacuum gauge located in the upper part. For the sake of clarity, the box and the sealing cap of the upper part of the cell are not illustrated.

system to the sample and protects it during its installation into the cell, and (3) a vacuum system that insulates the sample from the outside.

The first part, whose concept is close to that of the cell of *Pinzer and Schneebeli* [2009b], consists of two strictly identical assemblies that impose a vertical TG through the sample holder. Each assembly consists of a Peltier module (Kryotherm TB-2-(199-199)-0.8) in contact with two heat exchangers located at the cold and warm sides of the module. The exchangers are made of copper to facilitate the heat conduction. The temperatures of the cold heat exchangers of the system are measured using four-wire Pt100 temperature probes (IEC 60751-Class A) and regulated via a controller (Meerstetter TEC-1122). The Pt100 probes were calibrated together in a thermoregulated bath so that the accuracy on their temperature difference is below ± 0.02°C in the range [0, −20]°C. The temperature settings of the Peltier modules are ensured by the controller with a precision of about ± 0.01°C. The warm parts of the Peltier modules are continuously cooled by a water circulation at around 20°C through the warm heat exchangers to avoid overheating of the modules. The Peltier modules and the heat exchangers are grouped in a box where a slight dry air circulation flows continuously to prevent condensation or deposition of the ambient water vapor above the considered cold surfaces. The heat is conducted from the extremities of the CellDyM to the snow sample by a removable conduction system.

The conduction system consists of an aluminum cylinder inserted between two identical copper columns of 1.6 cm diameter and 14 cm height, which are themselves in contact with the cold heat exchangers. Their contact surfaces were finely polished to obtain a good thermal contact. The aluminum sample holder can contain a snow sample of 1 cm diameter and 1 cm height and conducts heat along the lateral sides of the sample. This lateral conduction contributes to obtain a uniform TG within the sample. As in the work of *Pinzer and Schneebeli* [2009b], aluminum was chosen for its relatively high thermal conduction and low X-ray absorption properties. The sample holder is of 3 cm height and of 0.3 cm thick, except at its central part where it is of 0.1 cm thick to minimize the absorption of the X-rays through the aluminum. It fits into each copper column along 1 cm to enhance the thermal conduction between the components and which also stabilizes the assembly. In addition, the external surfaces of the aluminum sample holder were polished to decrease the surface emissivity and limit the infrared radiation from the outside to the snow sample.

The third part of the CellDyM consists of a vacuum system that thermally insulates the snow sample from the tomograph room. For that, a Plexiglas cylinder of internal diameter of 4.4 cm surrounds the sample holder, creating a chamber. While the cell is operating, the air remaining in the chamber is permanently pumped at the base of the Plexiglas cylinder by a turbomolecular pump (Pfeiffer TMU065) connected to a membrane pump (Vacuubrand MZ2D). A Pirani gauge provides an estimation of the air pressure in the chamber by measuring the pressure via a short tube of 0.5 cm diameter placed at the upper part of the system. The measured pressure usually reaches values around 0.1 Pa quickly after starting the pumping system, leading to a thermal conductivity of air of around 0.0015 W $m^{-1}K^{-1}$ (reduced by $\sim$ 28 compared to that at atmospheric pressure). This value was estimated using the equation given by *Potkay et al.* [2007] and assuming that 0.1 Pa is representative of the pressure in the vacuum chamber. The tightness of the vacuum chamber is ensured by sealing caps equipped with O-rings, which connect the Plexiglas extremities to the cold heat exchangers, and by O-rings between the aluminum sample holder and the copper columns, which isolate the snow sample. The turbomolecular pump is connected to the vacuum chamber by around 30 cm of vacuum tube and cooled by a 20°C water circulation. The membrane pump is installed outside the tomograph cabin to prevent heating of the air and connected to the turbo pump by a flexible vacuum tube. Note that the Plexiglas cylinder of 5 cm external diameter constrains the distance between the X-ray source and the snow sample and thus might be a limitation for the pixel size in case of conical beams (minimum voxel size of 7 μm for the 3SR scanner; this value depends on the divergence of the X-ray beam).

3. Temperature Field Simulations

Measurements of temperature close to the snow sample are not performed since they are complex to design and may perturb locally the temperature field. We thus carried out a series of heat conduction simulations, using the finite element code ComsolMultiphysics, to evaluate the temperature field inside the cryogenic cell and the snow sample depending on the imposed thermal boundary conditions at the heat exchangers. All the components of the cell shown in Figure 1 were defined as an axisymmetric solid model. The thermal conductivity of copper (Cuc2, 99.99% minimum purity), aluminum (Aluminum 1350, 99.5% minimum purity), Plexiglas, and air at around 0.1 Pa were taken equal to 390, 200, 0.2, and 0.0015 W m^{-1} K^{-1}, respectively. In order to reflect the temperature field of the snow sample, we used an effective thermal conductivity corresponding to low-density snow of 0.2 W m^{-1} K^{-1} [*Calonne et al.*, 2011]. We imposed the temperatures of the heat exchangers at the top (T_{top}) and base (T_{base}) of the system, as well as the temperature of the tomograph cabin (T_{room}). The contacts between the different components were assumed to be perfect. The heat transfer by radiation and air convection were neglected.

Figure 1 shows two results of the temperature simulations of the snow sample. The left temperature field was simulated for isothermal conditions, with $T_{top} = T_{base} = -7$°C and $T_{room} = 20$°C. The latter temperature corresponds to the value $\pm$ 2°C measured in the cabin with a thermometer during the scans. The simulated field is slightly influenced by the outside with temperature values between −6.921 and −6.922°C, leading to a maximum temperature difference in the sample of 0.001°C. The analysis of the field leads to a maximum TG of the order of 0.2 K m^{-1}. This value is far below the minimal TG of 3 K m^{-1} for which temperature gradient effects can be observed [*Flin et al.*, 2007]. Under such conditions, the sample is thus expected to undergo isothermal metamorphism as presented, e.g., by *Kämpfer and Schneebeli* [2007].

The right temperature field of the sample shown in Figure 1 was simulated for TG conditions, where $T_{top} = -2.2$°C, $T_{base} = -1.8$°C, and $T_{room} = 20$°C. The TG between the two heat exchangers is thus 1.4 K m^{-1}. At the top and base of the snow sample, the temperatures are −2.034 and −1.910°C, respectively, leading to a local TG through the snow sample of 12 K m^{-1}. In practice, we use such simulations to determine the temperature settings to apply to the Peltier modules in order to impose a given local TG for our experiments. In the figure, the influence of the outside temperature is not observable on the field's shape: the isotherms in the sample are perpendicular to the gradient. Under such conditions, a uniform TG metamorphism is thus expected to occur.

4. Application to Snow Metamorphism

To check the accuracy of the CellDyM, time-lapse X-ray tomography was carried out at the 3SR laboratory to monitor the equitemperature metamorphism and the temperature gradient (TG) metamorphism of a snow

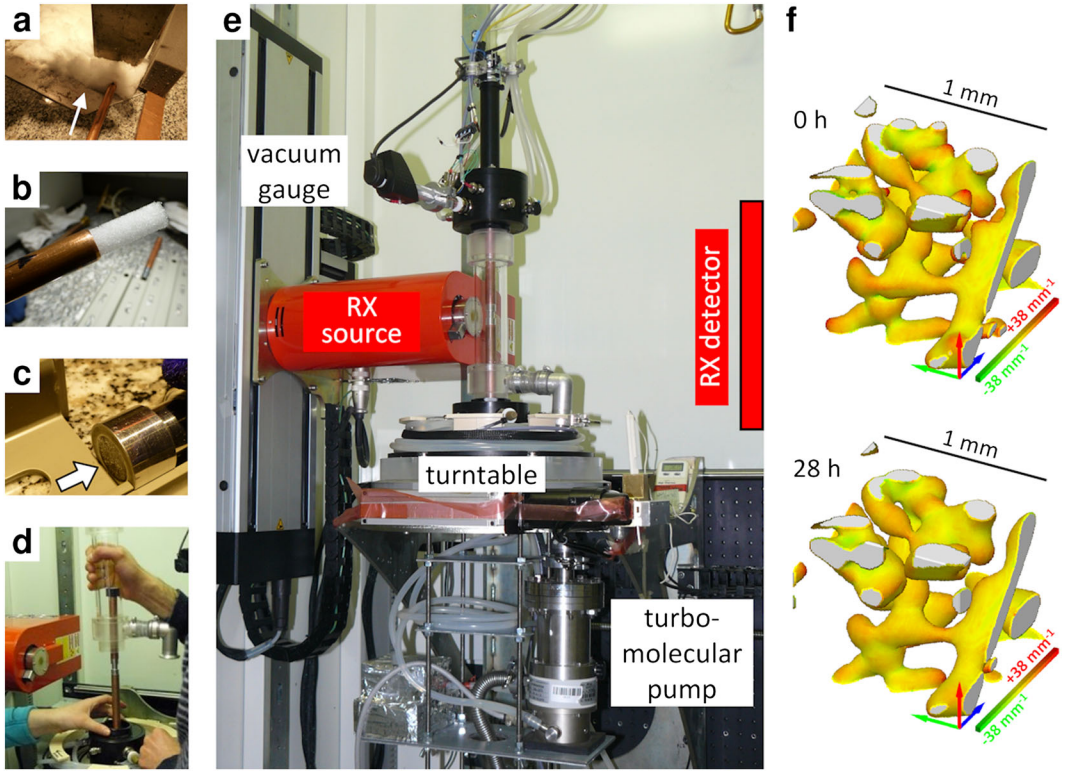


Figure 2. Photographs of the experiment and results for equitemperature metamorphism: (a) Snow coring into a snow layer; (b) Cylindrical snow sample; (c) Core insertion into the aluminum sample holder; (d) Installation of the sample into the cryogenic cell; (e) Overview of the CellDyM installed in the tomograph cabin (RX-solutions) of the 3SR lab. (f) A subvolume of the snow sample undergoing an equitemperature metamorphism at −7°C. The color map indicates the mean curvature scale, where convexities, flat shapes, and concavities are shown in red, yellow, and green, respectively. The red arrows are pointing downward of the physical sample. The voxel size is 7.8 μm.

sample. In what follows, we describe for both types of metamorphism the experimental process, from the sampling to the tomography, as well as the 3-D images and vertical cross sections obtained.

4.1. Equitemperature Metamorphism

The snow sample was prepared in cold room following the method below (see Figures 2a–2c for illustrations). First, two layers of ice of around 1.5 mm thickness were created at the extremity of the copper columns to provide a constant source (or sink) of water vapor over the metamorphism. A cylindrical snow core of 1 cm diameter and 0.7 cm height was sampled from a natural snow layer collected near Grenoble, France, consisting of decomposed and fragmented precipitation particles (DF) and rounded grains (RG) at around 160 kg m^{-3}. The aluminum sample holder was mounted on the lower copper column, ready to receive the snow sample. The sample was carefully inserted into the aluminum sample holder and then isolated from outside by fitting the upper copper column into the sample holder. The set was put in a copper holster and placed in isothermal conditions at −7°C in a freezer waiting for the tomography.

CellDyM was installed into the tomographic cabin (RX-solutions) as shown in Figure 2e. The turbomolecular pump was fixed below the turntable of the tomograph. CellDyM was screwed to the turntable via a platform where the water and air tubes of the lower part of the cell were initially wounded. Similarly, the tubes of the cell's upper part were initially twisted and attached at the top of the cabin. Indeed, both upper and lower tubes unwind during tomography, which facilitates the rotation process.

Before the sample installation, the temperatures of the upper and lower heat exchangers were both set to −7°C. The snow sample was set up in the CellDyM following a process where the aluminum sample holder is in direct contact with the ambient air for only few seconds (Figure 2d). Moreover, the copper columns constitute an important cold mass that protects the snow sample from heating. Immediately after, the vacuum pumping system was started and operated until the end of the experiment.

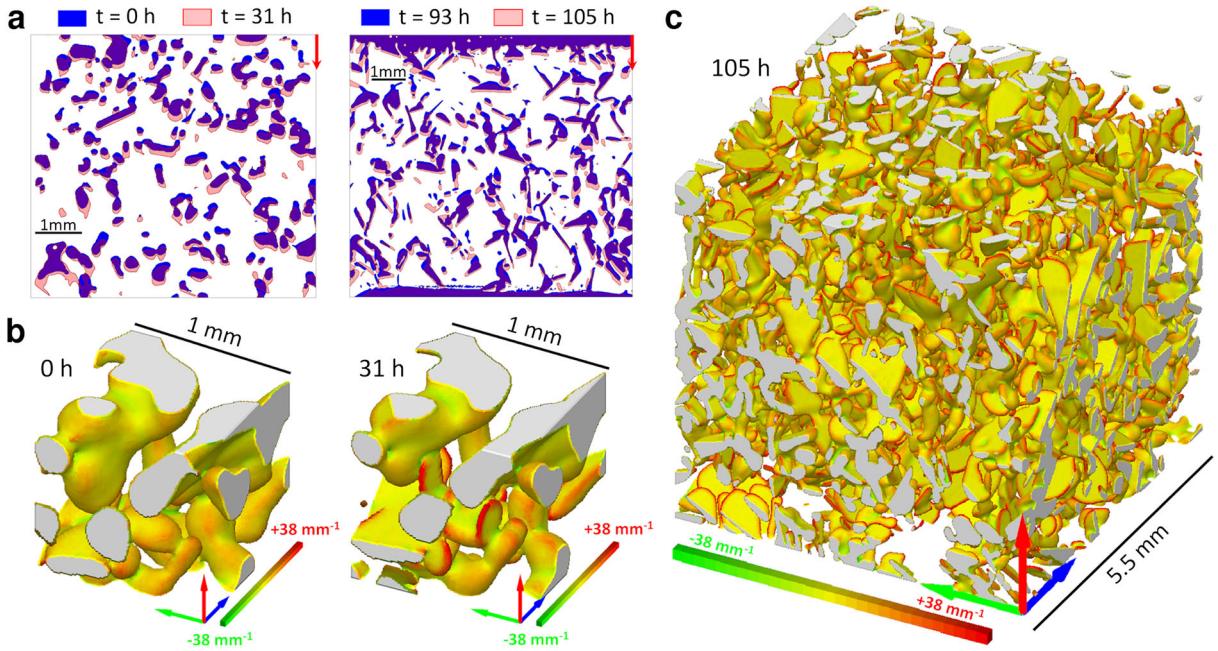


Figure 3. (a) Vertical cross sections, (b) subvolumes, and (c) whole volume of 3-D images of the snow sample undergoing a TG metamorphism of 18 K m^{-1} at −2°C for different times. All the red arrows are oriented toward the bottom of the physical sample. The left and right cross sections are represented using different magnifications. The 3-D images are colored with respect to the mean curvature scale and represented upside down for a better visualization of the facets. The voxel size is 7.8 μm.

We performed time-lapse tomography to monitor the equitemperature metamorphism of the prepared snow sample over 28 h. The temperature settings at the top and base of the cell were maintained at −7°C. The first tomography was started 1 h after the beginning of the isothermal conditions to ensure stabilized thermal conditions. Throughout the metamorphism, the snow sample was regularly scanned at a resolution of 7.8 μm via the software X-Act. We used a voltage of 80 kV and a current of 120 μA, for a scan duration of 2 h. These parameters ensure the best compromise between the quality of radiographs and the duration of the scan. Note that this latter should be defined depending on the rate of the sample evolution. The scan duration is not an issue with the equitemperature metamorphism, as its evolution is generally slow. We obtained 1200 radiographs per scan covering a 360° rotation around the vertical axis of the sample. The number of pixels of the X-ray detector was 1920 × 1536. The software DigiXCT was used to reconstruct horizontal cross sections of the snow samples from the radiographs. Three-dimensional binary images of around 6 × 6 × 6 mm^3 of the snow microstructure were finally obtained after image processing.

Figure 2f shows 1 × 1 × 1 mm^3 subvolumes of the snow sample at the beginning and after 28 h of equitemperature metamorphism. No significant changes occur during this period. Nevertheless, through a grain to grain comparison, the initial structure exhibits convex surfaces in red which are no longer present at t = 28 h, meaning that these surfaces have been preferentially sublimated. In the same time, the initial concave surfaces in green become less numerous at t = 28 h, which indicates that vapor deposition occurred in these areas. Qualitatively, the general evolution is a slight rounding of the ice structure, which is typical of the equitemperature metamorphism and in agreement with previous studies [*Flin et al.*, 2004; *Kämpfer and Schneebeli*, 2007]. This observation is in accordance with the simulated temperature field and validates the control of the TG through the sample.

4.2. Temperature Gradient Metamorphism

The preparation of the snow sample and its setting up into the CellDyM followed basically the same protocol presented in section 4.1. Time-lapse tomography was carried out to monitor the TG metamorphism of the prepared snow sample over 105 h. The temperature settings of the Peltier modules at the top and base were set to −2.2°C and −1.8°C, respectively. From similar simulations to those presented in section 3, but considering additional ice layers of thermal conductivity of 2.1 W m^{-1} K^{-1}, we estimated a local TG of 18 K m^{-1} through the sample. As for the equitemperature metamorphism, the first tomography was

started 1 h after setting the TG to ensure stabilized thermal conditions. The tomography parameters were the same as those given in section 4.1, the TG having been chosen sufficiently moderate to enable a 2 h duration scan.

The structural evolution of the snow sample is illustrated by vertical cross sections (Figure 3a) and $1\times1\times1$ mm^3 subvolumes of 3-D images (Figure 3b). The ice layers at the top and the bottom of the snow sample are visible in the right cross section. With time, the ice matrix appears to move gradually downward, with sublimation at the top and deposition at the bottom of the ice structures. The initial DF/RG evolves to faceted crystals (FC), characterized by faceted shapes and angular surfaces. Such planar or convex zones (yellow or red surfaces on 3-D images, respectively), can be easily detected after 31 h of TG. These observations are consistent with the simulated value of 18 K m^{-1} through snow, as well as with previous studies [e.g., *Flin and Brzoska*, 2008].

Figure 3c shows the final structure of the whole snow sample reached after 105 h of TG at an average temperature of −2°C. The ice structure exhibits several plate shapes indicating that the ice growth has been faster along preferential directions of the crystals. The observed shapes are in agreement with the ice crystal growth habits at −2°C. Indeed, at this temperature, the prismatic faces of the ice crystal grow faster than the basal faces, leading to plate-shaped crystals [*Kuroda and Lacmann*, 1982; *Furukawa and Wettlaufer*, 2007]. Moreover, we can notice that most of the "lateral" sides of the plates are rounded more than faceted. This observation is also a typical feature of the ice evolution just above −2°C and has been already reported by *Colbeck* [1983] and *Furukawa and Kohata* [1993]: close to the melting point, the basal faces of the crystals remain plane while the prismatic faces are rounded, even under a significant TG. The above considerations validate the temperature control of the CellDyM because the snow evolution is in agreement with the temperature conditions expected from simulations and also with the evolutions reported in the literature for similar conditions.

5. Conclusion and Outlooks

We developed a new cryogenic cell (CellDyM) that is suited to the dynamic monitoring of snow metamorphism, and which operates at room temperature. For this last reason, the CellDyM is adaptable to a large panel of tomographic scanners, including those of synchrotron instruments, which has several advantages in terms of speed, resolution, and imaging techniques [e.g., *Rolland du Roscoat et al.*, 2011; *Nguyen-Thi et al.*, 2012]. CellDyM controls precisely the temperature conditions at the boundaries of the sample by combining (1) a system of cold regulation and conduction that forces the temperature at the top and bottom of the sample, and (2) a vacuum system that insulates the sample from outside. Thus, the type and regime of metamorphism can be imposed on a snow sample over several days, making it possible to monitor its grain to grain evolution by time-lapse tomography at room temperature.

Experiments of equitemperature and TG metamorphisms were monitored using the CellDyM installed in the 3SR tomograph (RX-solutions). We obtained a time series of 3-D images for each experiment where the structural evolution of snow is observable at a 7.8 μm voxel size. A typical rounding of the shapes was observed during equitemperature metamorphism at −7°C, as reported in the literature [e.g., *Kämpfer and Schneebeli*, 2007] for diverse temperatures. TG metamorphism of 18 K m^{-1} at −2°C exhibited specific patterns of rounded plates, which constitutes the first 3-D record of the anisotropic behavior, in terms of faceting transition, between the basal (faceted) and prismatic faces (rounded) [*Colbeck*, 1983; *Furukawa and Kohata*, 1993]. All these observations are consistent with the temperature fields expected from heat conduction simulations and confirm the accuracy of the cell. They also clearly show that, at a precision of 7.8 μm, a period of about 30 h is long enough to observe measurable changes in snow microstructure, which confirms the interest of relatively short monitoring times (days) to study snow metamorphism. Further work will focus on the quantitative analysis of the above 3-D series to compute local growth rates and compare them to those predicted by microscale models.

Acknowledgments
Funding by Météo-France and Digital-Snow (ANR-11-BS02-009) is acknowledged. We thank F. Dominé for his contribution to the vacuum pumping system, G. Vian and F. Karmous for the machining of several elements of the cell, and M. Dumont for the study of the radiative energy balance of the vacuum chamber. CNRM-GAME/CEN is part of the LabEx OSUG@2020 (ANR-10-LABX-0056). The 3SR lab is part of the LabEx Tec 21 (Investissements d'Avenir, grant agreement ANR-11-LABX-0030). The 3-D images of Figures 2 and 3 can be obtained on request (frederic.flin@meteo.fr), after the signature of an agreement with Météo-France.

The Editor thanks Ian Baker and one anonymous reviewer for their assistance in evaluating this paper.

References

Brzoska, J.-B., C. Coléou, B. Lesaffre, S. Borel, O. Brissaud, W. Ludwig, E. Boller, and J. Baruchel (1999), 3D visualization of snow samples by microtomography at low temperature, *ESRF Newsletter*, *32*, 22–23.

Calonne, N., F. Flin, S. Morin, B. Lesaffre, S. R. du Roscoat, and C. Geindreau (2011), Numerical and experimental investigations of the effective thermal conductivity of snow, *Geophys. Res. Lett.*, *38*, L23501, doi:10.1029/2011GL049234.

Calonne, N., C. Geindreau, F. Flin, S. Morin, B. Lesaffre, S. Rolland du Roscoat, and P. Charrier (2012), 3-D image-based numerical computations of snow permeability: Links to specific surface area, density, and microstructural anisotropy, *The Cryosphere*, *6*(5), 939–951, doi:10.5194/tc-6-939-2012.

Calonne, N., F. Flin, C. Geindreau, B. Lesaffre, and S. Rolland du Roscoat (2014a), Study of a temperature gradient metamorphism of snow from 3-D images: Time evolution of microstructures, physical properties and their associated anisotropy, *The Cryosphere*, *8*(6), 2255–2274, doi:10.5194/tc-8-2255-2014.

Calonne, N., C. Geindreau, and F. Flin (2014b), Macroscopic modeling for heat and water vapor transfer in dry snow by homogenization, *J. Phys. Chem. B*, *118*(47), 13,393–13,403, doi:10.1021/jp5052535.

Chen, S., and I. Baker (2010), Evolution of individual snowflakes during metamorphism, *J. Geophys. Res.*, *115*, D21114, doi:10.1029/2010JD014132.

Colbeck, S. C. (1983), Ice crystal morphology and growth rates at low supersaturations and high temperatures, *J. Appl. Phys.*, *54*(5), 2677–2682.

Coléou, C., B. Lesaffre, J.-B. Brzoska, W. Ludwig, and E. Boller (2001), Three-dimensional snow images by X-ray microtomography, *Ann. Glaciol.*, *32*, 75–81, doi:10.3189/172756401781819418.

Enzmann, F., M. Miedaner, M. Kersten, N. V. Blohn, K. Diehl, S. Borrmann, M. Stampanoni, M. Ammann, and T. Huthwelker (2011), 3-D imaging and quantification of graupel porosity by synchrotron-based micro-tomography, *Atmos. Meas. Tech.*, *4*(10), 2225–2234.

Flin, F., and J.-B. Brzoska (2008), The temperature gradient metamorphism of snow: Vapour diffusion model and application to tomographic images, *Ann. Glaciol.*, *49*, 17–21, doi:10.3189/172756408787814834.

Flin, F., J.-B. Brzoska, B. Lesaffre, C. Coléou, and R. A. Pieritz (2003), Full three-dimensional modelling of curvature-dependent snow metamorphism: First results and comparison with experimental tomographic data, *J. Phys. D: Appl. Phys.*, *36*, A49–A54, doi:10.1088/0022-3727/36/10A/310.

Flin, F., J.-B. Brzoska, B. Lesaffre, C. Coléou, and R. A. Pieritz (2004), Three-dimensional geometric measurements of snow microstructural evolution under isothermal conditions, *Ann. Glaciol.*, *38*, 39–44, doi:10.3189/172756404781814942.

Flin, F., J.-B. Brzoska, R. Pieritz, B. Lesaffre, C. Coléou, and Y. Furukawa (2007), The temperature gradient metamorphism of snow: Model and first validations using X-ray microtomographic images, in *Proceedings of the 11th International Conference on the Physics and Chemistry of Ice held at Bremerhaven, Germany on 23–28 July 2006*, edited by W. Kuhs, pp. 181–189, Special Publication Nr 311, RSC, Cambridge, U. K.

Furukawa, Y., and S. Kohata (1993), Temperature dependence of the growth form of negative crystal in an ice single crystal and evaporation kinetics for its surfaces, *J. Cryst. Growth*, *129*, 571–581.

Furukawa, Y., and J. S. Wettlaufer (2007), Snow and ice crystals, *Phys. Today*, *60*(12), 70–71.

Grannas, A. M., et al. (2007), An overview of snow photochemistry: Evidence, mechanisms and impacts, *Atmos. Chem. Phys.*, *7*, 4329–4373.

Heggli, M., E. Frei, and M. Schneebeli (2009), Snow replica method for three-dimensional X-ray microtomographic imaging, *J. Glaciol.*, *55*(192), 631–639.

Kämpfer, T., and M. Schneebeli (2007), Observation of isothermal metamorphism of new snow and interpretation as a sintering process, *J. Geophys. Res.*, *112*, D24101, doi:10.1029/2007JD009047.

Kämpfer, T. U., and M. Plapp (2009), Phase-field modeling of dry snow metamorphism, *Phys. Rev. E*, *79* (3), 031502, doi:10.1103/PhysRevE.79.031502.

Kuroda, T., and R. Lacmann (1982), Growth kinetics of ice from the vapour phase and its growth forms, *J. Cryst. Growth*, *56*(1), 189–205.

Löwe, H., F. Riche, and M. Schneebeli (2013), A general treatment of snow microstructure exemplified by an improved relation for thermal conductivity, *The Cryosphere*, *7*(5), 1473–1480, doi:10.5194/tc-7-1473-2013.

Miedaner, M. M., T. Huthwelker, F. Enzmann, M. Kersten, M. Stampanoni, and M. Ammann (2007), X-ray tomographic characterization of impurities in polycrystalline ice, in *Proceedings of the 11th International Conference on the Physics and Chemistry of Ice held at Bremerhaven, Germany on 23–28 July 2006*, edited by W. Kuhs, pp. 399–407, Special Publication Nr 311, RSC Publishing, Cambridge, U. K.

Nguyen-Thi, H., L. Salvo, R. H. Mathiesen, L. Arnberg, B. Billia, M. Suery, and G. Reinhart (2012), On the interest of synchrotron X-ray imaging for the study of solidification in metallic alloys, *C. R. Phys.*, *13*(3), 237–245.

Pinzer, B., and M. Schneebeli (2009a), Snow metamorphism under alternating temperature gradients: Morphology and recrystallization in surface snow, *Geophys. Res. Lett.*, *36*, L23503, doi:10.1029/2009GL039618.

Pinzer, B., and M. Schneebeli (2009b), Breeding snow: An instrumented sample holder for simultaneous tomographic and thermal studies, *Meas. Sci. Technol.*, *20*(9), 095705.

Pinzer, B., M. Schneebeli, and T. Kämpfer (2012), Vapor flux and recrystallization during dry snow metamorphism under a steady temperature gradient as observed by time-lapse micro-tomography, *The Cryosphere*, *6*, 1141–1155.

Potkay, J. A., G. R. Lambertus, R. D. Sacks, and K. D. Wise (2007), A low-power pressure- and temperature-programmable micro gas chromatography column, *J. Microelectromech. Syst.*, *16*(5), 1071–1079.

Riche, F., and M. Schneebeli (2013), Thermal conductivity of snow measured by three independent methods and anisotropy considerations, *The Cryosphere*, *7*(1), 217–227, doi:10.5194/tc-7-217-2013.

Rolland du Roscoat, S., A. King, A. Philip, P. Reischig, W. Ludwig, F. Flin, and J. Meyssonnier (2011), Analysis of snow microstructure by means of X-ray diffraction contrast tomography, *Adv. Eng. Mater.*, *13*(3), 128–135, doi:10.1002/adem.201000221.

Schneebeli, M., and S. A. Sokratov (2004), Tomography of temperature gradient metamorphism of snow and associated changes in heat conductivity, *Hydrol. Processes*, *18*(18), 3655–3665, doi:10.1002/hyp.5800.

Schweizer, J., J. B. Jamieson, and M. Schneebeli (2003), Snow avalanche formation, *Rev. Geophys.*, *41*(4), 1016, doi:10.1029/2002RG000123.

Sokratov, S. A., and R. G. Barry (2002), Intraseasonal variation in the thermoinsulation effect of snow cover on soil temperatures and energy balance, *J. Geophys. Res.*, *107*(D10), 4093, doi:10.1029/2001JD000489.

Srivastava, P., P. Mahajan, P. Satyawali, and V. Kumar (2010), Observation of temperature gradient metamorphism in snow by X-ray computed microtomography: Measurement of microstructure parameters and simulation of linear elastic properties, *Ann. Glaciol.*, *51*(54), 73–82.

Zermatten, E., S. Haussener, M. Schneebeli, and A. Steinfeld (2011), Tomography-based determination of permeability and Dupuit-Forchheimer coefficient of characteristic snow samples, *J. Glaciol.*, *57*(205), 811–816, doi:10.3189/002214311798043799.

Zermatten, E., M. Schneebeli, H. Arakawa, and A. Steinfeld (2014), Tomography-based determination of porosity, specific area and permeability of snow and comparison with measurements, *Cold Reg. Sci. Technol.*, *97*, 33–40, doi:10.1016/j.coldregions.2013.09.013.